



浙江海洋大學
ZHEJIANG OCEAN UNIVERSITY

7th International Conference on Tethers in Space

June 2-5, 2024, York University, Toronto, Canada

Velocity Observer Design of Space Tether System using Immersion and Invariance technique

Jihang Yang¹, Yonghe Xie¹, Gangqiang Li²

¹ School of Naval Architecture and Maritime, Zhejiang Ocean University, Zhoushan, China

² École Centrale Nantes, CNRS, LHEEA, UMR 6598, F-44000 Nantes, France

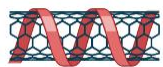
Contents



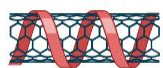
The Research Background



System Description



Simulation Results



Conclusions and Future Work

The Research Background



Fig. 1 Image of TISS-1
(USA & Canada)



Fig. 2 Image of STARS
(Japan)

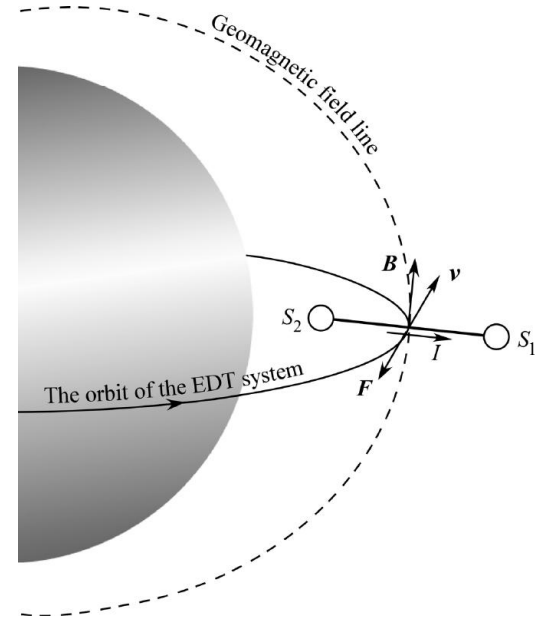


Fig. 3 Scheme of tethered
spacecraft system

The Research Background

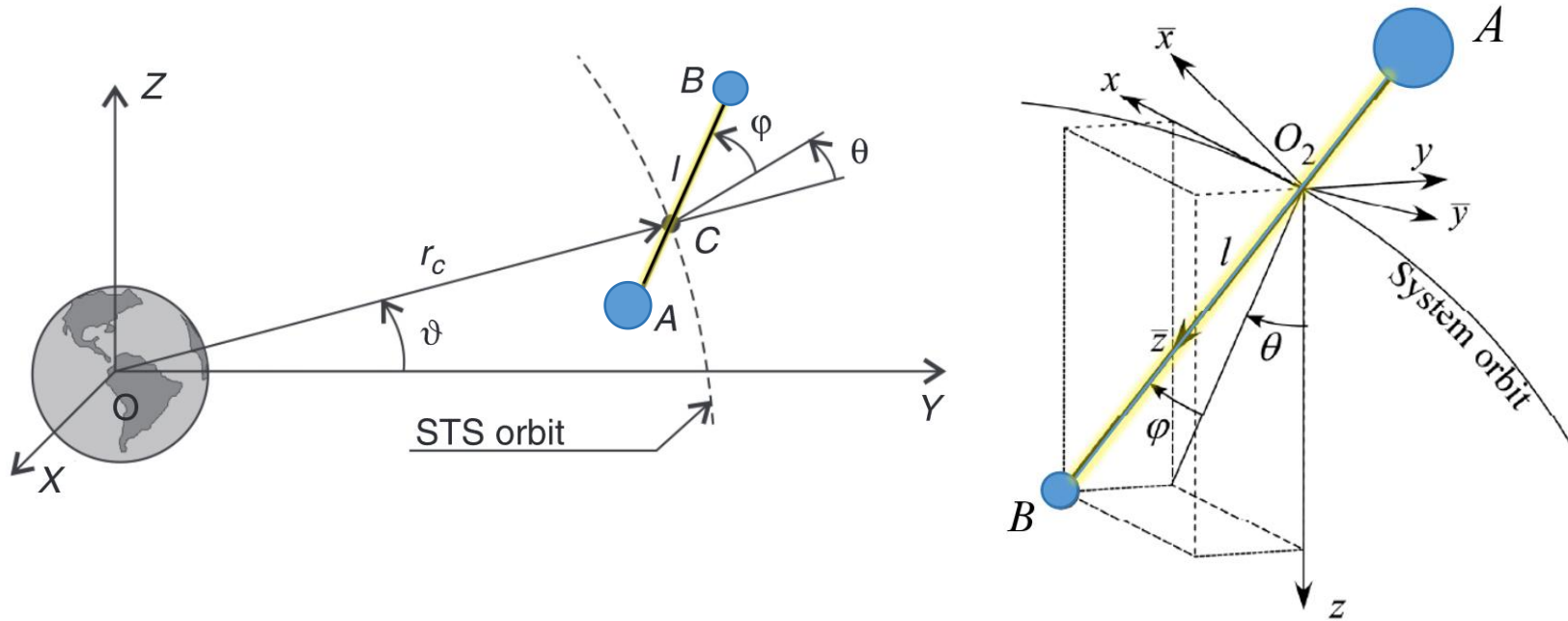


Fig 4. Scheme of space tether system.

Motivation

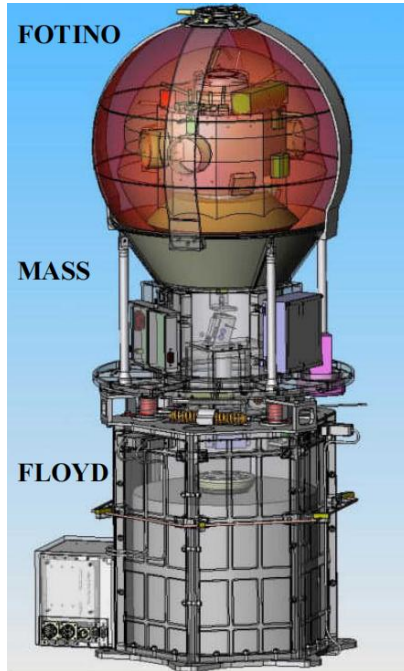


Fig 5. YES2 contains FLOYD , MASS and Fotino, the spherical re-entry capsule.

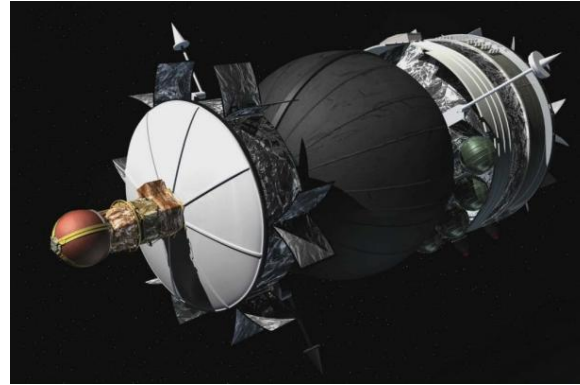


Fig 6. YES2 on Foton.

Problem

Velocity filter overestimated the speed in the first minute after ejection, leading the controller to command additional braking, which lead to a decrease of velocity.

- [1] Kruijff, M., Summary of Data Analysis of the YES2 Tethered SpaceMail Experiment, Delft University of Technology, 2008.
- [2] I.V. Belokonov, M.V. Bondar, I.A. Kudryavtsev, Problems of Navigational Support of a Tether System Deployment by an Example of the YES2 Experiment Aboard Foton M3, 1 (2010).

Motivation

the Kalman filter algorithm

- [3] T.S. Denney, M.E. Greene, **On state estimation for an orbiting single tether system**, IEEE Trans. Aerosp. Electron. Syst. 27 (1991) 689–695. <https://doi.org/10.1109/7.85043>.
- [4] P. Williams, **Electrodynamic Tethers Under Forced-Current Variations Part II: Flexible-Tether Estimation and Control**, J. Spacecr. Rockets 47 (2010) 320–333.
- [5] G. Li, Z.H. Zhu, **Estimation of flexible space tether state based on end measurement by finite element Kalman filter state estimator**, Adv. Space Res. 67 (2021) 3282–3293. <https://doi.org/10.1016/j.asr.2021.01.057>.
- [6] P. Tortora, L. Somenzi, L. Iess, R. Licata, **Small Mission Design for Testing In-Orbit an Electrodynamic Tether Deorbiting System**, J. Spacecr. Rockets 43 (2006) 883–892. <https://doi.org/10.2514/1.15359>.

Estimate the **unmeasure states** of the tether system

In [6], Tortora et al. designed an extended Kalman filter to estimate the in-plane and out-of-plane libration angles and **angular velocities** for Space Tether attitude control.

A significant computational source is required to process a set of sampling points (sigma points).

Methodology - Immersion and Invariance (I&I) Technique

- [7] Ø.N. Starnes, O.M. Aamo, G.-O. Kaasa, A constructive speed observer design for general Euler–Lagrange systems, *Automatica* 47 (2011) 2233–2238. <https://doi.org/10.1016/j.automatica.2011.08.006>.
- [8] A. Astolfi, D. Karagiannis, R. Ortega, *Nonlinear and Adaptive Control with Applications*, Springer London, London, 2008. <https://doi.org/10.1007/978-1-84800-066-7>.
- [9] A. Astolfi, R. Ortega, A. Venkatraman, A Globally Exponentially Convergent Immersion and Invariance Speed Observer for N Degrees of Freedom Mechanical Systems, Proc. 48h IEEE Conf. Decis. Control CDC Held Jointly 2009 28th Chin. Control Conf. (2009) 6508–6513. <https://doi.org/DOI: 10.1109/CDC.2009.5399984>.



➔ **the in-plane pitch angle θ and out-of-plane roll angle ϕ**

- [10] H. Wen, Z.H. Zhu, D. Jin, H. Hu, Exponentially Convergent Velocity Observer for an Electrodynamic Tether in an Elliptical Orbit, *J. Guid. Control Dyn.* 39 (2016) 1113–1118. <https://doi.org/10.2514/1.G001532>.

I&I adaptive Control
Nonlinear Observer Design

- Electrical System
- Mechanical System
- Electromechanical System

Methodology - Immersion and Invariance (I&I) Technique

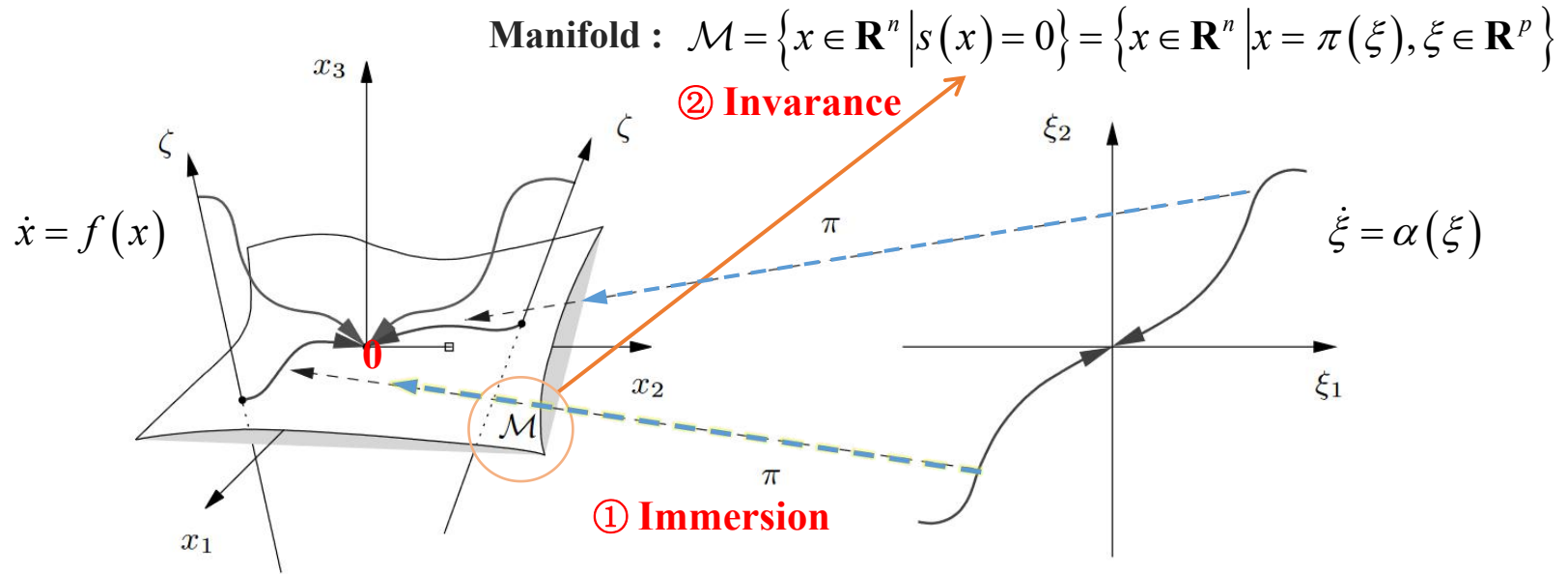
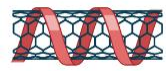
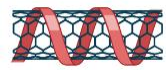


Fig. 5 Graphical illustration of the mapping between the trajectories of the system to be controlled and the target system.

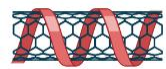
Contents



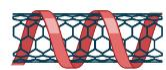
The Research Background



System Description



Simulation Results



Conclusions and Future Work

System Description

The dynamic equations of the space tether system during the deployment

$$l'' - l \left[(\theta' + \Omega)^2 + \Omega^2 (3 \cos^2 \theta - 1) \right] = -\frac{\bar{T}}{m_0} \quad (1)$$

$$l^2 \theta'' + 2ll' (\Omega + \theta') + \frac{3}{2} l^2 \Omega^2 \sin 2\theta = 0$$

Define the following nondimensional variables:

$$\lambda = l/l_n, \quad \tilde{T} = \bar{T}/(m_0 l_n \Omega^2), \quad \tau = \Omega t, \quad \dot{s} = ds/dt \quad (2)$$

The nondimensional equations of tethered system (1) can be presented as following

$$\ddot{\lambda} - \lambda \left[(\dot{\theta} + 1)^2 - 1 + 3 \cos^2 \theta \right] = -\tilde{T} \quad (3)$$

$$\lambda^2 \ddot{\theta} + 2\lambda\dot{\lambda} (1 + \dot{\theta}) + 3\lambda^2 \sin \theta \cos \theta = 0$$

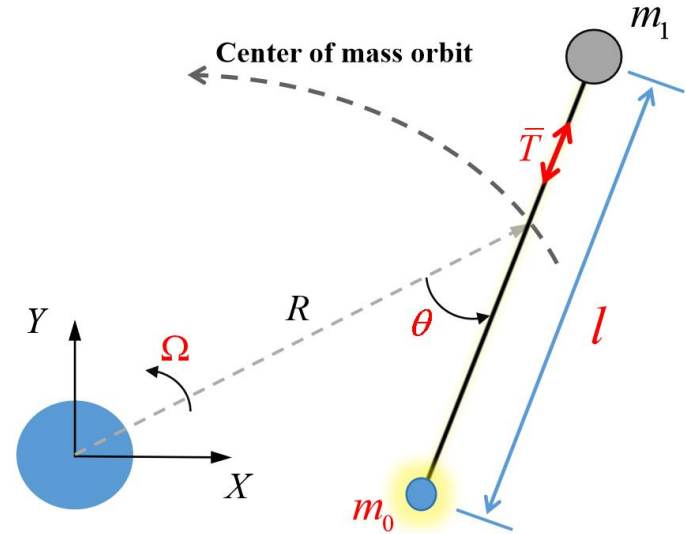
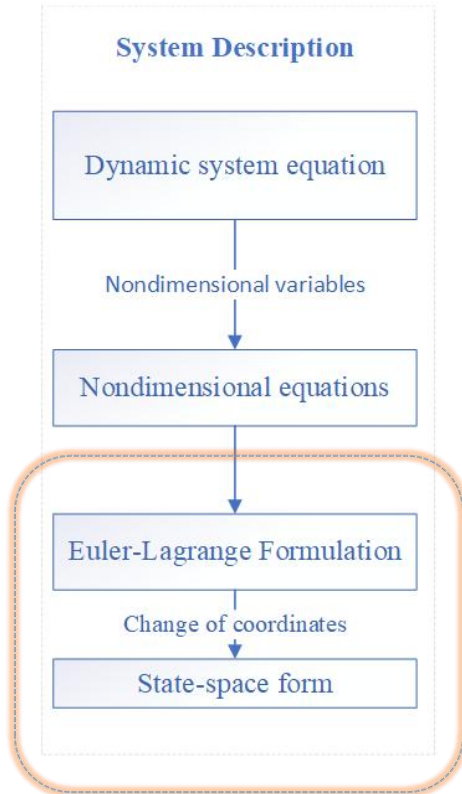


Fig. 6 Schematic diagram of STS

System Description



Furthermore, the system can be described in Euler-Lagrange by

$$M(q)\ddot{q} + C(q, \dot{q})\dot{q} + G(q) = u \quad (4)$$

where $q = [\lambda \ \theta]^\top$, $u = [-\tau \ 0]^\top$, $M(q) = M^\top(q) > 0$

Then, a **factorization** of the generalized inertia matrix is used as

$$M(q) = T^\top(q)T(q), \quad T(q) = \begin{bmatrix} 1 \\ \lambda \end{bmatrix} \quad (5)$$

And the change of coordinates $(\dot{q} \ q)^\top \mapsto (x \ y)^\top$

where $x = T(q)\dot{q}$, $y = q$

Define the mapping and as $L(q) = T^{-1}(q)$, $F(q, u) = T^{-\top}(q)(u - G(q))$ (6)

Therefore, the system (3) allows to be converted to a state-space form

$$\dot{y} = L(y)x \quad (7)$$

$$\dot{x} = S(x, y)x + F(y, u) \quad (8)$$

System Description - Velocity Observer Design

Main Result

Proposition 1. An exponentially convergent speed observer is designed for the STS (2) as follows, and are the observer states.

$$\begin{aligned} \dot{\eta} = & S_1(\eta + \beta, y) \cdot (\eta + \beta) + S_2 \cdot (\eta + \beta) + F(y, u) - \frac{\partial \beta}{\partial y} L(y) \cdot (\eta + \beta) - \frac{\partial \beta}{\partial \hat{y}} \dot{y} - \frac{\partial \beta}{\partial \hat{x}} \dot{x} \\ & - r^2 \left[\frac{\partial \beta}{\partial y} L(y) \right]^T e_x - r^2 L^T(y) e_y \end{aligned} \quad (12)$$

And the observer state $\hat{y}, \hat{x} \in \mathbb{R}^2$ obtained from the filter

$$\dot{\hat{y}} = L(y)(\eta + \beta) - \varphi_1 e_y \quad (13)$$

$$\dot{\hat{x}} = S_1(\eta + \beta, y) \cdot (\eta + \beta) + S_2 \cdot (\eta + \beta) + F(y, u) - \varphi_2 e_x - r^2 \left[\frac{\partial \beta}{\partial y} L(y) \right]^T e_x - r^2 L^T(y) e_y \quad (14)$$

where $\varphi_1 : \mathbb{R}^2 \times \mathbb{R}_+ \rightarrow \mathbb{R}_+$ and $\varphi_2 : \mathbb{R}^2 \times \mathbb{R}_+ \rightarrow \mathbb{R}_+$ are gain functions, the mapping $\beta \in \mathbb{R}^{2 \times 2} \rightarrow \mathbb{R}^2$ is an intermediate variable, which is defined below, and e_x, e_y are the error of the system state.

System Description

Observer Design

Define a manifold for system

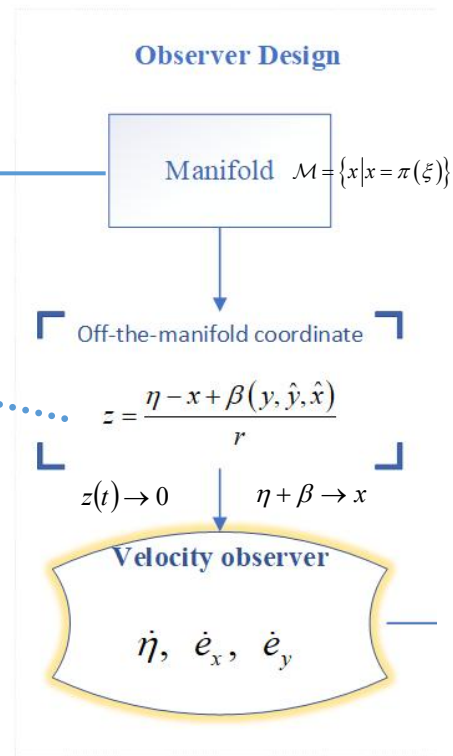
$$\pi := \{(y, x, \eta, \hat{y}, \hat{x}) : \eta + \beta(y, \hat{y}, \hat{x}) - x = 0\} \subset \mathbb{R}^2 \quad (15)$$

Then give the off-the-manifold coordinate

$$z = \frac{\eta - x + \beta(y, \hat{y}, \hat{x})}{r} \quad (16)$$

Differentiate the aforementioned equation, yields

$$\begin{aligned} \dot{z} &= \frac{[\dot{\eta} - \dot{x} + \dot{\beta}(y, \hat{y}, \hat{x})]r - \dot{r}[\eta - x + \beta(y, \hat{y}, \hat{x})]}{r^2} \\ &= \frac{\dot{\eta} - S_1(x, y)x - S_2x - F(y, u) + \nabla_y \beta \cdot L(y) \cdot x + \nabla_{\hat{y}} \beta \dot{\hat{y}} + \nabla_{\hat{x}} \beta \dot{\hat{x}}}{r} \\ &= -\frac{\dot{r}}{r} z \end{aligned} \quad (17)$$



System Description - Velocity Observer Design

Assigning

$$\begin{aligned} \dot{\eta} = & F(y, u) - \frac{\partial \beta}{\partial y} L(y) \cdot (\eta + \beta) - \frac{\partial \beta}{\partial \hat{y}} \dot{y} - \frac{\partial \beta}{\partial \hat{x}} \dot{x} + S_2 \cdot (\eta + \beta) \\ & + S_1(\eta + \beta, y) \cdot (\eta + \beta) - r^2 \left[\frac{\partial \beta}{\partial y} L(y) \right]^T e_x - r^2 L^T(y) e_y \end{aligned} \quad (18)$$

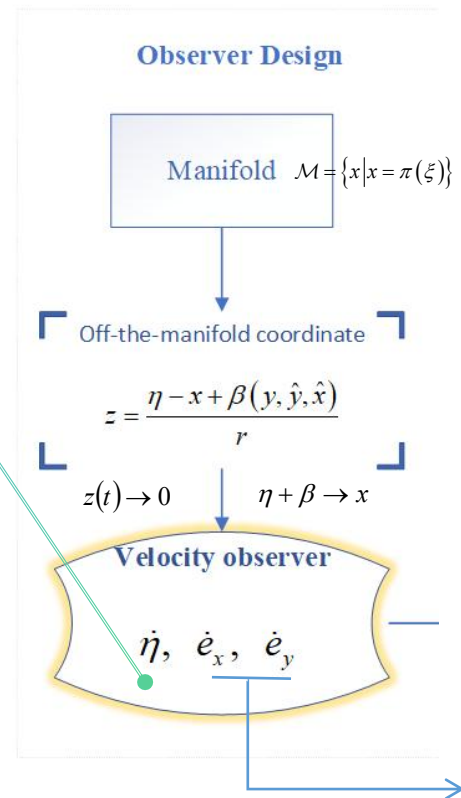
Meanwhile, defining the errors of the states x and y

$$e_y = \hat{y} - y \quad (19)$$

$$e_x = \hat{x} - \eta - \beta \quad (20)$$

Replacing equation (18) in (17), and using the *lemma 1*, yields

$$\begin{aligned} \dot{z} = & \frac{\dot{\eta} - S_1(x, y) \cdot x - S_2 \cdot x - F(y, u) + \nabla_y \beta L(y) \cdot x + \nabla_{\hat{y}} \beta \dot{y} + \nabla_{\hat{x}} \beta \dot{x}}{r} - \frac{\dot{r}}{r} z \\ = & S_1(x, y) \cdot z + \bar{S}_1(\eta + \beta, y) \cdot z + S_2 \cdot z - \frac{\partial \beta}{\partial y} L(y) \cdot z - r \left[\frac{\partial \beta}{\partial y} L(y) \right]^T e_x \\ & - r L^T(y) e_y - \frac{\dot{r}}{r} z \end{aligned} \quad (21)$$



System Description

Differentiate equations (19) and (20), respectively,

$$e_y = \hat{y} - y \quad (19)$$

$$e_x = \hat{x} - \eta - \beta \quad (20)$$

$$\begin{aligned} \dot{e}_y &= \dot{\hat{y}} - \dot{y} = L(y) \cdot (\eta + \beta) - \varphi_1 e_y - L(y)x \\ &= L(y) \cdot (\eta + \beta) - L(y) \cdot (\eta + \beta - rz) - \varphi_1 e_y \\ &= L(y) \cdot rz - \varphi_1 e_y \end{aligned} \quad \begin{array}{l} \hookrightarrow \\ \hookrightarrow \end{array} \quad \begin{aligned} \dot{\hat{y}} &= L(y)(\eta + \beta) - \varphi_1 e_y \\ x &= \eta + \beta - rz \end{aligned} \quad (22)$$

meanwhile, substituting $\dot{\hat{x}}$ (14) and $\dot{\eta}$ (18) in differential (20), yields

$$\dot{e}_x = \dot{\hat{x}} - \dot{\eta} - \dot{\beta} = \frac{\partial \beta}{\partial y} L(y) \cdot rz - \varphi_2 e_x \quad (23)$$

The error system can be expressed in general Hamiltonian frame, with

$$H(z, e_y, e_x) = \frac{1}{2} z^\top z + \frac{1}{2} e_y^\top e_y + \frac{1}{2} e_x^\top e_x$$

$$\begin{bmatrix} \dot{z} \\ \dot{e}_y \\ \dot{e}_x \end{bmatrix} = \begin{bmatrix} S_1(x, y) & -rL^\top(y) & -r(\nabla_y \beta L(y))^\top \\ L(y)r & 0 & 0 \\ \nabla_y \beta L(y)r & 0 & 0 \end{bmatrix} \begin{bmatrix} \frac{\partial H}{\partial z} \\ \frac{\partial H}{\partial e_y} \\ \frac{\partial H}{\partial e_x} \end{bmatrix} - \begin{bmatrix} -\bar{S}_1(\eta + \beta, y) - S_2 + \nabla_y \beta L(y) + \frac{\dot{r}}{r} & 0 & 0 \\ 0 & \varphi_1 & 0 \\ 0 & 0 & \varphi_2 \end{bmatrix} \begin{bmatrix} \frac{\partial H}{\partial z} \\ \frac{\partial H}{\partial e_y} \\ \frac{\partial H}{\partial e_x} \end{bmatrix} \quad (24)$$

System Description

Define the partial differential equation (PDE) 

$$\frac{\partial \beta}{\partial y} = \nabla_y \beta = \bar{S}_1(\hat{x}, \hat{y}) L^\dagger(\hat{y}) + k_1 L^\dagger(\hat{y}) \quad (25)$$

$$\beta = \bar{S}_1(\hat{x}, \hat{y}) L^\dagger(\hat{y}) \cdot y + k_1 L^\dagger(\hat{y}) \cdot y \quad (26)$$

let the error mapping

$$\begin{aligned} \Delta &= \Delta_x(y, \hat{x}, e_x) + \Delta_y(y, \hat{x}, e_y) \\ &= \bar{S}_1(\eta + \beta, y) - \bar{S}_1(\hat{x}, \hat{y}) + [\bar{S}_1(\hat{x}, \hat{y}) + k_1 I] [L^\dagger(y) - L^\dagger(\hat{y})] L(y) + S_2 \end{aligned} \quad (27)$$

which are satisfied with $\Delta_x(y, \hat{x}, 0) = 0, \Delta_y(y, \hat{x}, 0) = 0$

the Hamiltonian function (24) can be transformed into

$$\begin{bmatrix} \dot{z} \\ \dot{e}_y \\ \dot{e}_x \end{bmatrix} = \begin{bmatrix} S_1(x, y) & -rL^\top(y) & -r(\nabla_y \beta L(y))^\top \\ L(y)r & 0 & 0 \\ \nabla_y \beta L(y)r & 0 & 0 \end{bmatrix} \begin{bmatrix} \frac{\partial H}{\partial z} \\ \frac{\partial H}{\partial e_y} \\ \frac{\partial H}{\partial e_x} \end{bmatrix} - \begin{bmatrix} k_1 I - \Delta + \frac{\dot{r}}{r} & 0 & 0 \\ 0 & \varphi_1 & 0 \\ 0 & 0 & \varphi_2 \end{bmatrix} \begin{bmatrix} \frac{\partial H}{\partial z} \\ \frac{\partial H}{\partial e_y} \\ \frac{\partial H}{\partial e_x} \end{bmatrix} \quad (28)$$

System Description - Velocity Observer Design

Stability

Proposition 2. Assume the scaling factor

$$\dot{r} = -\frac{k_1}{4}(r-1) + \frac{r}{2k_1}\|\Delta\|^2, \quad r(0) \geq 1 \quad (29)$$

and notice the factor r satisfied $\{r \in \mathbb{R} | r \geq 1\}$ and $k_1 > 0$

Proof:

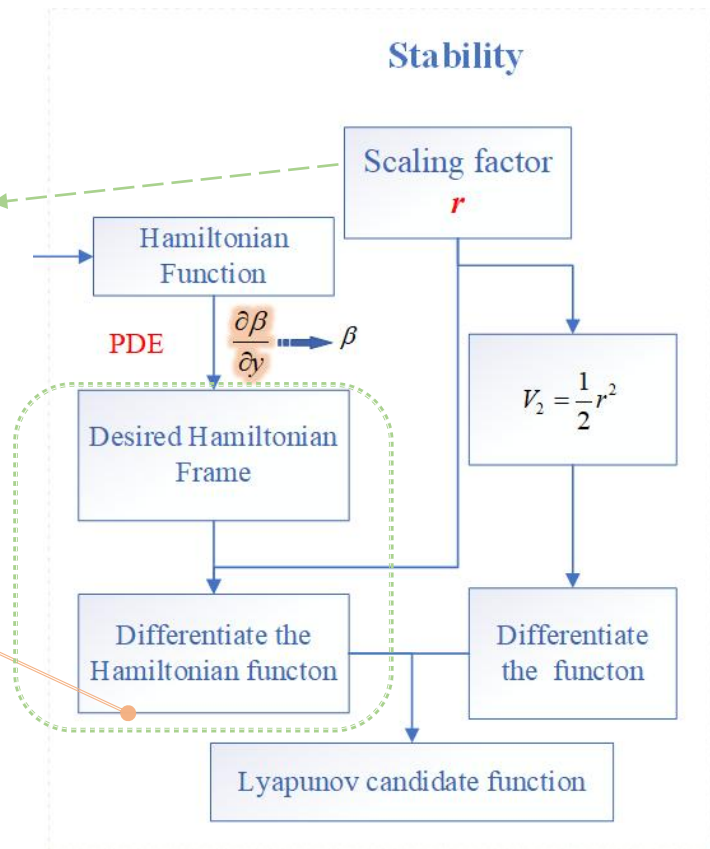
Step 1. (proof of stability of the general Hamiltonian function)

$$\dot{H}(z, e_y, e_x) = -z^\top \left(k_1 I - \Delta + \frac{\dot{r}}{r} \right) z - e_y^\top \varphi_1 e_y - e_x^\top \varphi_2 e_x \quad (30)$$

satisfies the property of $k_1 I - \Delta + \dot{r}/r \geq 0$

$$\text{get } \dot{H}(z, e_y, e_x) \leq 0 \quad (31)$$

when $\{z, e_y, e_x \in \mathbb{R}^n | \dot{H}(z, e_y, e_x) = 0\} = \{z, e_y, e_x | z = 0, e_y = 0, e_x = 0\}$



System Description - Velocity Observer Design

Select the positive-definite function

$$V_1 = \frac{1}{2} z^T z$$

and its derivative is

$$\dot{V}_1 = -z^T \left(k_1 I - \Delta + \frac{\dot{r}}{r} \right) z = -k_1 z^T z + z^T \Delta z - \frac{\dot{r}}{r} |z|^2 \quad (32)$$

According to the Young's inequality, yields

$$z^T \Delta z \leq \frac{k_1}{2} |z|^2 + \frac{1}{2k_1} \|\Delta\|^2 |z|^2$$

Therefore

$$\begin{aligned} \dot{V}_1 &= -z^T \left(k_1 I - \Delta + \frac{\dot{r}}{r} \right) z = -k_1 z^T z + z^T \Delta z - \frac{\dot{r}}{r} |z|^2 \\ &\leq -k_1 |z|^2 + \left(\frac{k_1}{2} |z|^2 + \frac{1}{2k_1} \|\Delta\|^2 |z|^2 \right) - \frac{\dot{r}}{r} |z|^2 = -\frac{k_1}{2} |z|^2 + \frac{1}{2k_1} \|\Delta\|^2 |z|^2 - \frac{\dot{r}}{r} |z|^2 \\ &\leq -\frac{k_1}{2} |z|^2 + \frac{k_1 (r-1)}{4r} |z|^2 \end{aligned} \quad (33)$$

$(r-1)/r \leq 1$



$$\dot{H}(z, e_y, e_x) = -z^T \left(k_1 I - \Delta + \frac{\dot{r}}{r} \right) z - e_y^T \varphi_1 e_y - e_x^T \varphi_2 e_x = V_1 - e_y^T \varphi_1 e_y - e_x^T \varphi_2 e_x \leq 0$$

System Description - Velocity Observer Design

Step 2. (proof of stability of the extended system) Select the proper Lyapunov candidate function for the extended system such that

$$V(z, e_y, e_x, r) = H(z, e_y, e_x) + V_2 = \frac{1}{2}z^\top z + \frac{1}{2}e_y^\top e_y + \frac{1}{2}e_x^\top e_x + \frac{1}{2}r^2 \quad (34)$$

Then, the derivative of the function

$$\begin{aligned} \dot{V}(z, e_y, e_x, r) &\leq -\frac{k_1}{4}|z|^2 - e_y^\top \varphi_1 e_y - e_x^\top \varphi_2 e_x + r\dot{r} \\ &= -\frac{k_1}{4}|z|^2 - e_y^\top \varphi_1 e_y - e_x^\top \varphi_2 e_x - \frac{k_1}{4}(r^2 - r) + \frac{r^2}{2k_1} \|\Delta\|^2 \\ &\leq -\frac{k_1}{4}|z|^2 - \varphi_1 e_y^2 - \varphi_2 e_x^2 - \frac{k_1}{4}(r^2 - r) + \frac{r^2}{k_1} \|\Delta_y\|^2 + \frac{r^2}{k_1} \|\Delta_x\|^2 \\ &\leq -k_1|z|^2 - \bar{\varphi}_1 e_y^2 - \bar{\varphi}_2 e_x^2 - \frac{k_1}{4}(r^2 - r) \end{aligned}$$

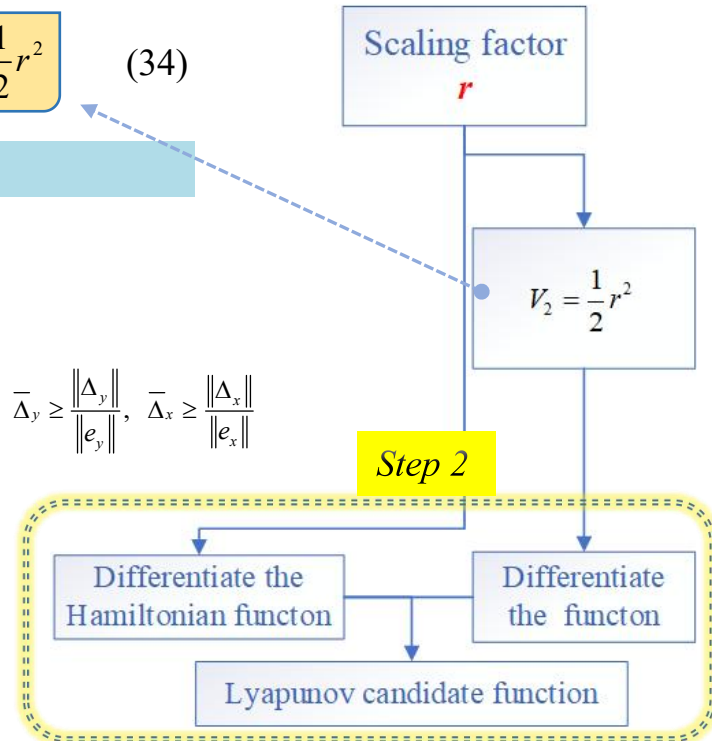
$$\bar{\Delta}_y \geq \frac{\|\Delta_y\|}{\|e_y\|}, \quad \bar{\Delta}_x \geq \frac{\|\Delta_x\|}{\|e_x\|}$$

Therefore

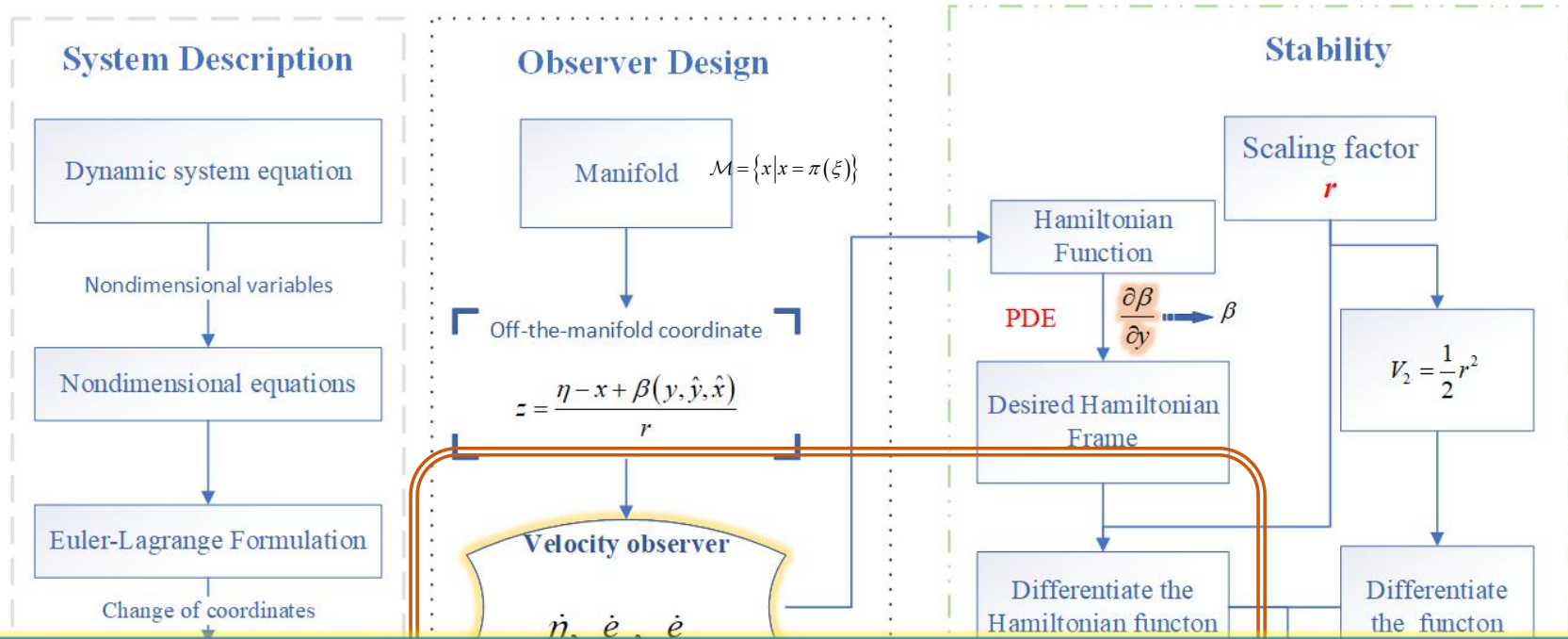
$$\dot{V}(z, e_y, e_x, r) \leq 0$$

$$r^2 - r \geq 0, r(0) \geq 1$$

Stability



System Description



Stabilisation via I&I is related to passivity-based stabilisation methods, with suitable storage function.

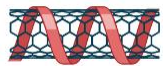
Contents



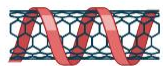
The Research Background



System Description



Simulation Results



Conclusions and Future Work

Simulation Results

Proposition 1.

$$\dot{\eta} = S_1(\eta + \beta, y) \cdot (\eta + \beta) + S_2 \cdot (\eta + \beta) + F(y, u) - \frac{\partial \beta}{\partial y} L(y) \cdot (\eta + \beta)$$

$$-\frac{\partial \beta}{\partial \hat{y}} \dot{\hat{y}} - \frac{\partial \beta}{\partial \hat{x}} \dot{\hat{x}} - r^2 \left[\frac{\partial \beta}{\partial y} L(y) \right]^\top e_x - r^2 L^\top(y) e_y$$

$$\dot{\hat{y}} = L(y)(\eta + \beta) - \varphi_1 e_y$$

$$\dot{\hat{x}} = S_1(\eta + \beta, y) \cdot (\eta + \beta) + S_2 \cdot (\eta + \beta) + F(y, u) - \varphi_2 e_x - r^2 \left[\frac{\partial \beta}{\partial y} L(y) \right]^\top e_x - r^2 L^\top(y) e_y$$

Input	Simulation parameters and initial conditions	
$u = [-\tau \quad 0]^\top$ $= [-3y_1 \cos^2 y_2 \quad 0]^\top$	$k_1 = 5, k_2 = 10$ $y_1(0) = 0.01, y_2(0) = 0$ $\hat{q}_1(0) = 0.05, \hat{q}_2(0) = 0$ $\eta_1(0) = 0.74, \eta_2(0) = 0$	$\bar{\varphi}_1 = \bar{\varphi}_2 = 0.175$ $x_1(0) = 0.5, x_2(0) = 0$ $\hat{x}_1(0) = 0.75, \hat{x}_2(0) = 0$ $r(0) = 1.5$

Simulation Results

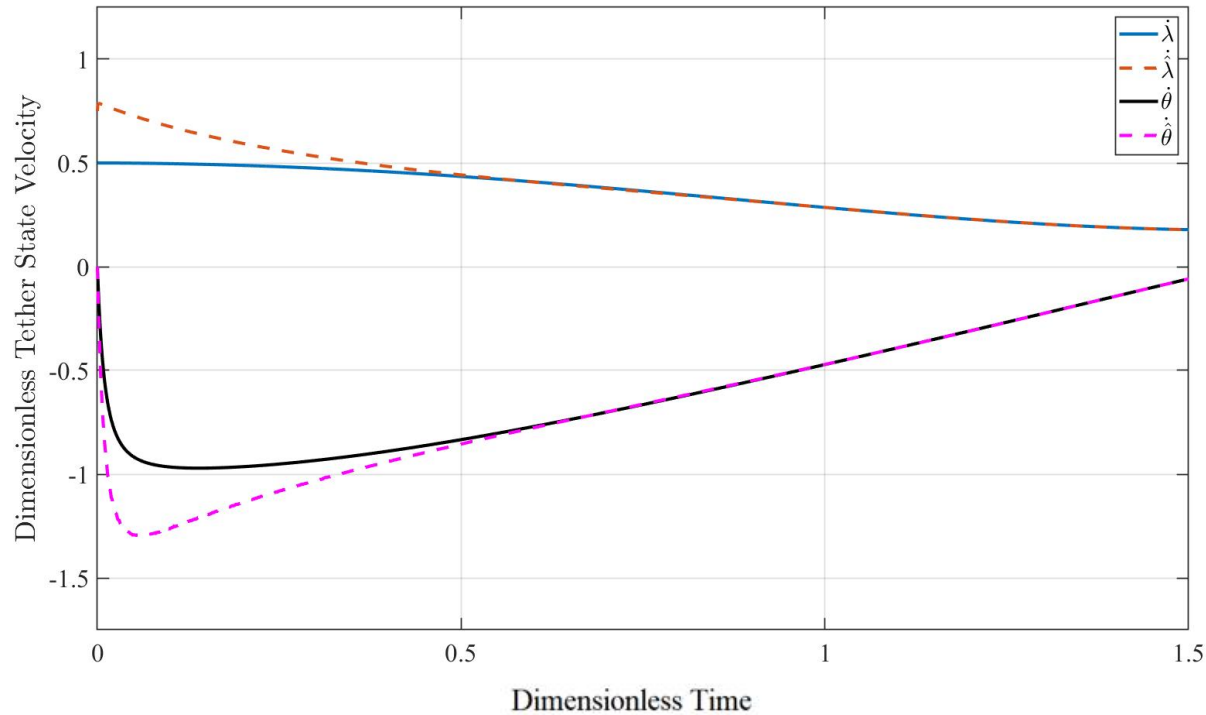


Fig. 7 Dimensionless time histories of comparison between **real velocities** $(\dot{\lambda}, \dot{\theta})$ and **estimated velocities** $(\hat{\lambda}, \hat{\theta})$.

Simulation Results

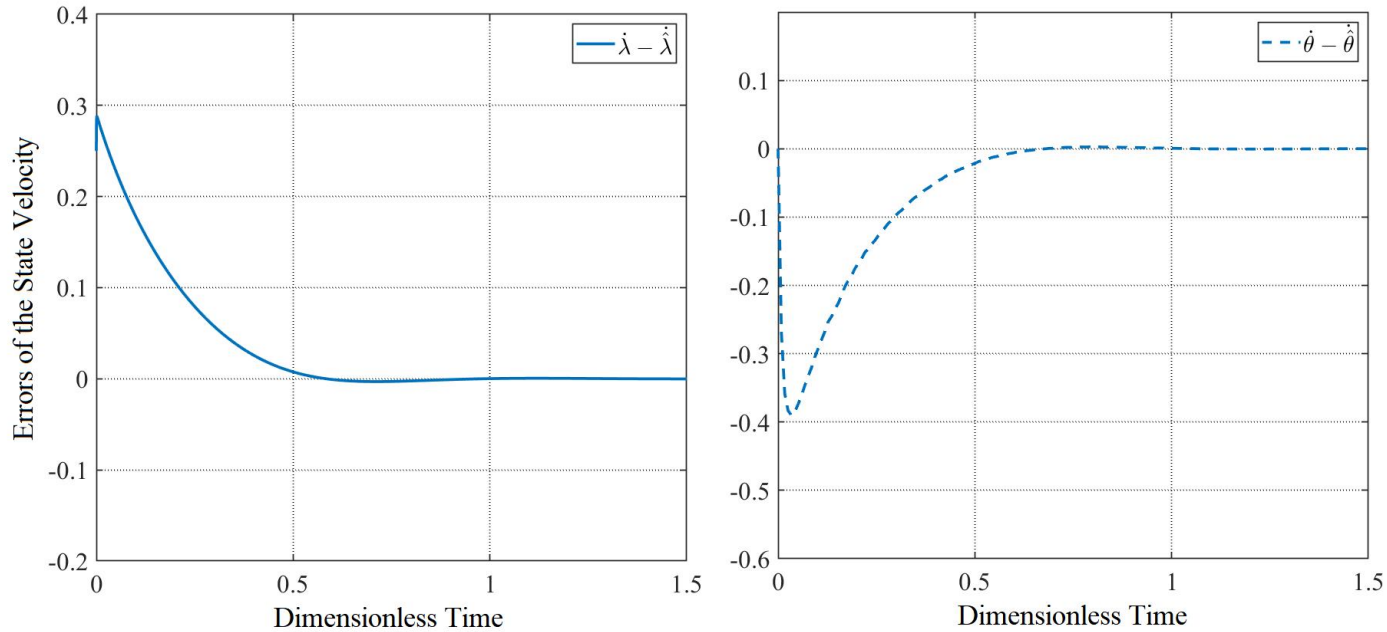


Fig. 2 Dimensionless time histories of the error between the real velocities and the estimated velocities

Simulation Results

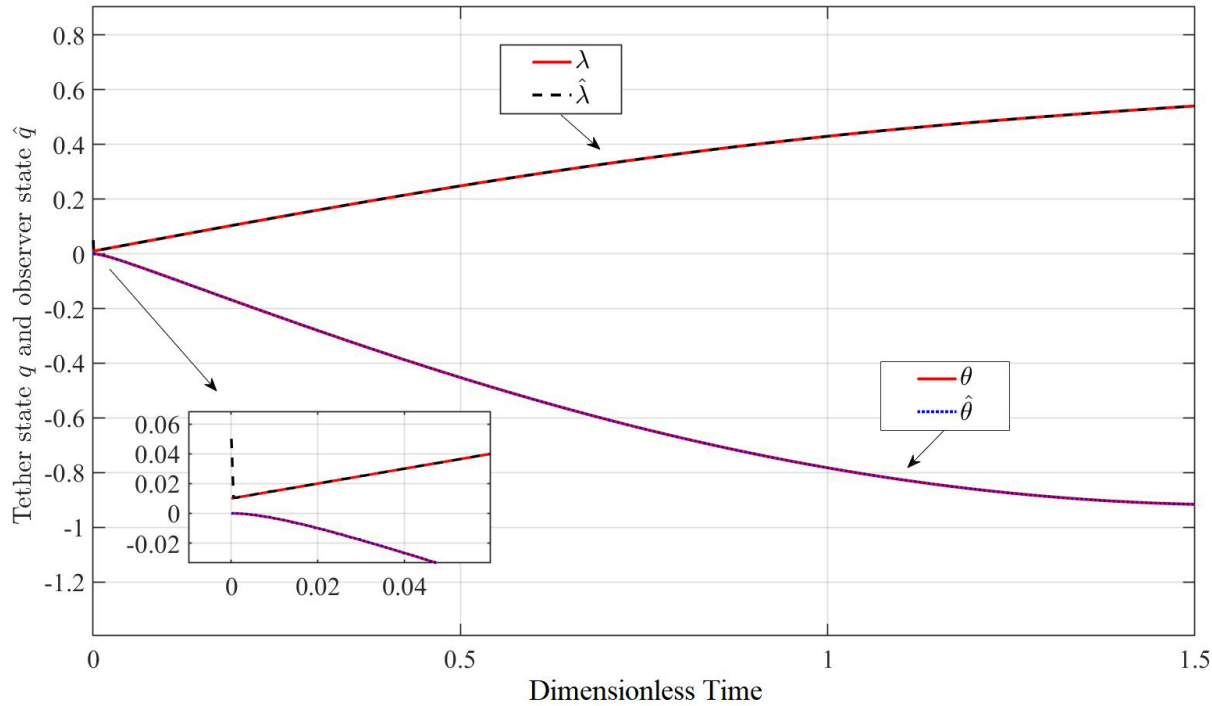


Fig.8 Dimensionless time histories of the comparison between $y = q = (\lambda \ \theta)^\top$ and $\hat{y} = \hat{q} = (\hat{\lambda} \ \hat{\theta})^\top$.

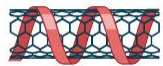
Contents



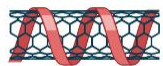
The Research Background



System Description



Simulation Results



Conclusions and Future Work



Conclusions



A nonlinear velocity observer to estimate the in-plane deployment velocities of the space tether system has been presented in this paper.



A crucial PDE



The stability analysis of the proposed velocity observer can be demonstrated based on the Hamiltonian principle

Future Work



Add perturbation to the the measured signals.

Thank you for listening !